Genetic Characterization of Mutants Resistant to the Antiauxin p-Chlorophenoxyisobutyric Acid Reveals That AAR3, a Gene Encoding a DCN1-Like Protein, Regulates Responses to the Synthetic Auxin 2,4-Dichlorophenoxyacetic Acid in Arabidopsis Roots[1][C][W]

Kamal Kanti Biswas[2], Chiharu Ooura[3], Kanako Higuchi, Yuji Miyazaki, Vinh Van Nguyen[4], Abidur Rahman[5], Hirofumi Uchimiya, Tomohiro Kiyosue, Tomokazu Koshiba, Atsushi Tanaka, Issay Narumi, and Yutaka Oono*

Radiation-Applied Biology Division, Japan Atomic Energy Agency, Takasaki 370–1292, Japan (K.K.B., V.V.N., A.R., A.T., I.N., Y.O.); Advanced Science Research Center, Japan Atomic Energy Research Institute, Takasaki 370–1292, Japan (C.O., H.U., Y.O.); Department of Biological Sciences, Graduate School of Science, Tokyo Metropolitan University, Hachioji, Tokyo 192–0397, Japan (K.H., T. Koshiba); United Graduate School of Agricultural Sciences, Ehime University, Matsuyama, Ehime 790–8566, Japan (Y.M., T. Kiyosue); Biology Department, University of Massachusetts, Amherst, Massachusetts 01003 (A.R.); Institute of Molecular and Cellular Biosciences, University of Tokyo, Tokyo 113–0032, Japan (H.U.); and Institute of Research Promotion, Kagawa University, Kagawa 761–0795, Japan (T. Kiyosue)

To isolate novel auxin-responsive mutants in Arabidopsis (*Arabidopsis thaliana*), we screened mutants for root growth resistance to a putative antiauxin, p-chlorophenoxyisobutyric acid (PCIB), which inhibits auxin action by interfering the upstream auxin-signaling events. Eleven PCIB-resistant mutants were obtained. Genetic mapping indicates that the mutations are located in at least five independent loci, including two known auxin-related loci, *TRANSPORT INHIBITOR RESPONSE1* and Arabidopsis *CULLIN1*. *antiauxin-resistant* mutants (*aar*s) *aar3-1*, *aar4*, and *aar5* were also resistant to 2,4-dichlorophenoxyacetic acid as shown by a root growth assay. Positional cloning of *aar3-1* revealed that the *AAR3* gene encodes a protein with a domain of unknown function (DUF298), which has not previously been implicated in auxin signaling. The protein has a putative nuclear localization signal and shares homology with the DEFECTIVE IN CULLIN NEDDYLATION-1 protein through the DUF298 domain. The results also indicate that PCIB can facilitate the identification of factors involved in auxin or auxin-related signaling.

The plant hormone auxin elicits a multitude of developmental and physiological responses, all of which are mediated by complex signaling pathways, throughout the plant life cycle (Leyser, 2002). Our knowledge concerning the mechanisms of auxin action has been substantially advanced by identification of several proteins that participate in the main events of auxin-stimulated Aux/IAA protein degradation (Leyser, 2002). The whole degradation mechanism is centered on the SCF^TIR1 ubiquitin E3 ligase complex. Auxin directly binds to the TRANSPORT INHIBITOR RESPONSE1 (TIR1) protein, a subunit of the SCF^TIR1 complex; stimulates its interaction with Aux/IAA proteins; and promotes Aux/IAA protein degradation (Dharmasiri et al., 2005a; Kepinski and Leyser, 2005). TIR1-related proteins, AFBs (auxin-signaling F-box proteins), also interact with Aux/IAA and, together with TIR1, mediate auxin responses throughout plant development (Dharmasiri et al., 2005b). However, the regulatory system of the TIR1/AFB pathway and whether the TIR1/AFB pathway accounts for all auxin responses largely remain unclear. Thus, it is possible that other uncharacterized proteins are involved in

SCF$^{\text{TIR1/AFB}}$-dependent or -independent auxin-signaling pathways.

Considering the absolute necessity of auxin for embryogenesis, it may be difficult to identify the genes that are related to such processes by screening auxin responses in seedlings. Recently, a new approach using a combination of forward and chemical genetics has emerged. In this approach, new mutants are screened against the endogenous or exogenous chemicals that presumably inhibit auxin signaling, because identifying the molecular targets of these compounds may help to reveal the mode of action of auxin as well as the upstream signaling events (Hayashi et al., 2003; Armstrong et al., 2004; Weijers and Jürgens, 2004; Surpin et al., 2005; Yamazoe et al., 2005).

We previously showed that p-chlorophenoxyisobutyric acid (PCIB) inhibits root growth, lateral root formation, root gravitropism, and the upstream auxin signaling events (Oono et al., 2003). These results prompted us to design a new mutant screening assay for identifying novel factors involved in upstream auxin-signaling pathways. By this screening, we successfully isolated an antiauxin-resistant1 (aar1) mutant that is specifically resistant to 2,4-dichlorophenoxyacetic acid (2,4-D) yet responds to other auxins like the wild type. Molecular characterization of aar1 further revealed that the 2,4-D sensitivity of the plants was conferred by SMALL ACIDIC PROTEIN1 (SMAP1), which works upstream in auxin-signaling pathways (Rahman et al., 2006). In this study, we report the isolation and characterization of additional PCIB-resistant mutants. We identified at least five independent loci, including two known auxin-related loci, TIR1 and Arabidopsis (Arabidopsis thaliana) CULLIN1 (AtCUL1), and three additional auxin-related mutants, aar3, aar4, and aar5. Positional cloning of aar3 showed that a gene encoding a DEFECTIVE IN CULLIN NEDDYLATION-1 (DCN-1)-like protein regulates the 2,4-D response in Arabidopsis roots. These results confirm that the mutant screening approach with PCIB has the potential to discover new factors involved in auxin-related signaling pathways.

RESULTS

Effect of PCIB on Arabidopsis Root Growth

To explore the effect of PCIB on root growth, wild-type Arabidopsis seedlings were grown vertically in the presence or absence of 20 μM PCIB (Fig. 1). Root growth of wild-type Arabidopsis seedlings began to slow down at 5 to 6 d and almost ceased at 10 d (Figs. 1A and 3B). Confocal images with propidium iodide indicated that PCIB inhibited root growth by reducing the size of the root meristem (Fig. 1B). The number of cortical cells in the meristematic zone in PCIB-treated roots [17.4 ± 3.6 (SD)] was significantly less than that in the control roots (30.6 ± 6.5). Moreover, the expression pattern of DR5::GUS, an auxin response marker (Ulmasov et al., 1997), was significantly reduced in

the root tip of 5-d-old seedlings grown on 20 μM PCIB (Fig. 1, C and D). However, the levels of free indole-3-acetic acid (IAA) in 3-mm root tips of control and PCIB-treated seedlings were indistinguishable (Table I). The results suggested that the reduction of meristem size in PCIB-treated roots is probably due to the reduced auxin response by PCIB rather than a reduced IAA level. However, we cannot completely rule out the possibility that the reduced meristem size was due to decreased auxin content as the auxin content of 3-mm root tips may not be representative of the auxin content in meristems that are only 500 μm in length.

Long-term incubation (10–14 d) in PCIB (10–20 μM PCIB) induced a dramatic change in root morphology (Fig. 1, E–G). Active cell division was observed in the upper meristem region in 10-d-old seedlings, preceding the new secondary meristem initiation from the lateral side of the primary original meristem. The secondary meristems grew much faster than the primary meristem, expanded in a lateral direction, and produced an increased number of epidermal cell files, resulting in the formation of secondary roots (Fig. 1, E–G; data not shown). A broad GUS activity in marker lines for quiescent centers (QCs; QC46 and QC25; Sabatini et al., 1999) was detected inside the columella tissue of secondary roots (Fig. 1E, arrowhead for QC46; data not shown for QC25). The starch grains that are characteristic of columella were also detected in the outermost layer of secondary roots (Fig. 1F, arrowhead). The free IAA content was 1.4 times higher in the root tips of PCIB-treated seedlings than in the controls (Table I), consistent with a strong DR5::GUS expression in the secondary root meristem (Fig. 1G).

Isolation and Genetic Analyses of the aar Mutants

On the basis of root growth data (Fig. 1), we screened mutants from 2-week-old M$_2$ seedlings grown vertically in the presence of 20 μM PCIB and established 11 PCIB-resistant lines by repeatedly testing for a PCIB response over several generations. After mapping or sequence analyses (described below), several mutant lines were given aar designations due to their independent loci. Homozygous lines for aar1-1, aar2-1, aar3-1, aar4, aar5, m31, and m34 were successfully established. m35, m36, m85, and m100 could be maintained only as heterozygotes. All mutant lines, except aar1-1, were backcrossed with the wild type, and scored for root length in the F$_1$ and F$_2$ generations (Table II). Characterization of aar1 was published elsewhere (Rahman et al., 2006). Based on the segregation ratio, we concluded that aar2-1 is a single semidominant mutant; aar3-1 and aar4 are single recessive mutants; and aar5, m31, and m34 are dominant mutants. Seedlings derived from self-fertilization of the PCIB-resistant m35 and m36 segregated in 1 (PCIB-sensitive):2 (PCIB-resistant) ratios. However, crosses between the wild type and these mutant lines produced a ratio of 1:1 for PCIB-sensitive and PCIB-resistant seedlings,
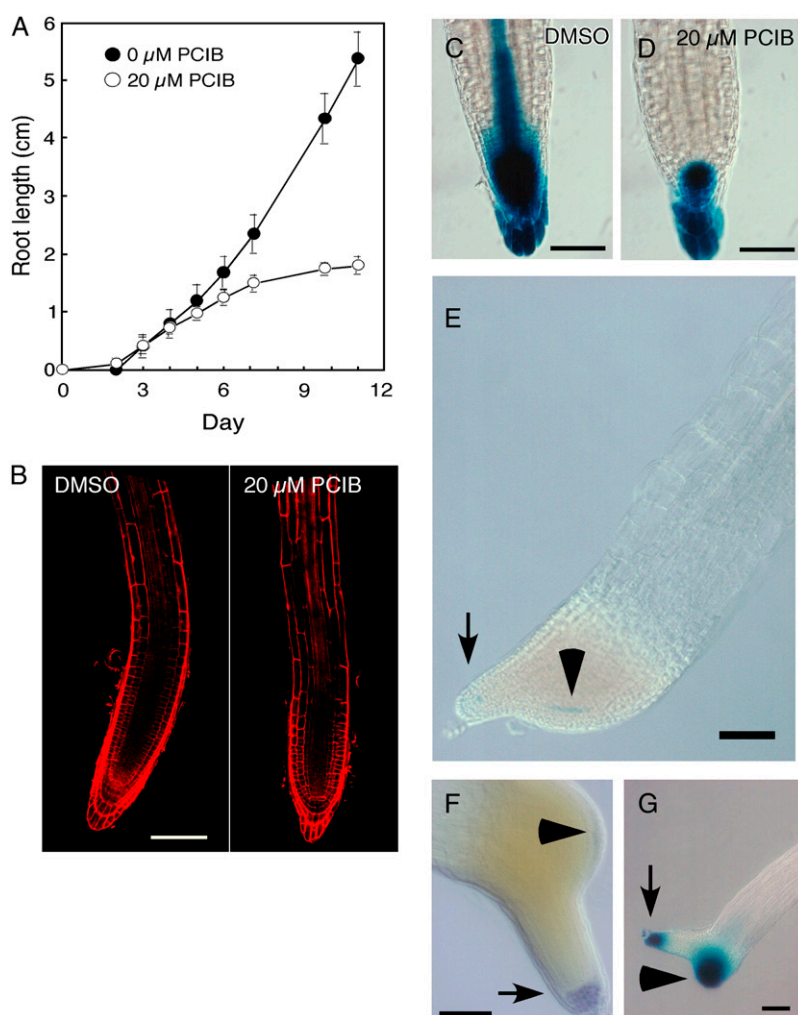
Figure 1. Effects of PCIB on root growth and root tip morphology of Arabidopsis. A, Wild-type (Columbia-0) seedlings ($n = 14$) were germinated on GM with or without 20 μM PCIB and grown vertically under continuous light. Error bars indicate SD. Absence of bars indicates deviation is less than size of symbol. B, Roots from 5-d-old wild-type seedlings germinated and horizontally grown on GM with (right) or without (left) 20 μM PCIB were stained with 10 μg/mL propidium iodide. Bar = 100 μm. C and D, Roots from 5-d-old *DR5::GUS* seedlings germinated and grown vertically on GM without (C) or with (D) 20 μM PCIB were stained with X-gluc for 15 h. Bar = 50 μm. E, A root from a 10-d-old QC46 seedling germinated and grown vertically on GM containing 20 μM PCIB was stained with X-gluc for 15 h. Arrow indicates primary root tip. Arrowhead indicates QC cells in secondary meristem. Bar = 100 μm. F, A root from a 14-d-old wild-type seedling germinated and grown vertically on GM containing 20 μM PCIB was stained with Lugol's solution (Merck KGaA) to visualize starch granules and was cleared with chloral hydrate (Willemsen et al., 1998). Arrow indicates primary root tip. Arrowhead indicates starch granules in the newly formed columella cells in secondary meristem. Bar = 100 μm. G, A root from a 10-d-old *DR5::GUS* seedling germinated and vertically grown on GM with 20 μM PCIB was stained with X-gluc for 15 h. Arrow indicates original distal root tip. Arrowhead indicates secondary root meristem. Bar = 100 μm.

which suggests that these mutations are dominant and may be homozygous lethal. Self-crossing of mutant lines *m85* and *m100* resulted in a 1 (PCIB-sensitive):1 (PCIB-resistant) segregation ratio. When each of these mutant lines (female) was crossed with wild-type pollen, both PCIB-sensitive and PCIB-resistant seedlings appeared in the next generation and they segregated in an approximately 2 (PCIB-sensitive):1 (PCIB-resistant) ratio. Cross-pollination of pollen from these mutants to wild-type stigma failed to produce any PCIB-resistant seedlings in the next generation. These results suggest that the *m85* and *m100* mutations do not transfer through male gametophytes, but are partially inherited through female gametophytes.

Mapping of the *aar* Mutations and Identification of *TIR1* and *AtCUL1* Alleles

The chromosomal positions of these mutations were determined using simple sequence length polymorphism and cleaved amplified polymorphic sequence markers (Fig. 2A), with the exception of *aar2-1*, which was isolated from a T-DNA-mutagenized seedling population.

Table I. *Effect of PCIB on total free IAA content in Arabidopsis root apical segments*[a]

Treatment	IAA Content in Apical Root Section	
	5-d-Old Apical 3 mm	10-d-Old Apical 5 mm
	pg/mg fresh weight	
Untreated	19.81 ± 3.71	18.25 ± 1.13
20 μM PCIB	20.27 ± 4.01	25.94 ± 6.26**

[a]Data are means ± SD. *P* value was obtained by Student's *t* test for control versus PCIB-treated plants. **, $P < 0.01$.

Table II. *Genetic analysis of Arabidopsis aar mutants*

Genotype of Parents (Female × Male)		Progeny			χ^{2a} (Hypothesis)
		PCIB Sensitive	PCIB Resistant		
AAR2/AAR2 × aar2/aar2	F$_2$	57	(weak)	(strong)	1.73 (1:2:1)
			111	45	
aar3/aar3 × AAR3/AAR3	F$_1$	77	0		–
	F$_2$	70	24		0.01 (3:1)
aar4/aar4 × AAR4/AAR4	F$_1$	60	0		–
	F$_2$	42	19		1.23 (3:1)
aar5/aar5 × AAR5/AAR5	F$_1$	0	42		–
	F$_2$	28	70		0.67 (1:3)
m31/m31 × M31/M31	F$_1$	0	63		–
	F$_2$	26	84		0.11 (1:3)
m34/m34 × M34/M34	F$_1$	0	69		–
	F$_2$	32	92		0.04 (1:3)
m35/M35 × m35/M35	Self	32	85		1.89 (1:2)
m35/M35 × M35/M35	F$_1$	27	29		0.07 (1:1)
m36/M36 × m36/M36	Self	44	101		0.58 (1:2)
m36/M36 × M36/M36	F$_1$	35	37		0.06 (1:1)
m85/M85 × m85/M85	Self	55	68		1.38 (1:1)
m85/M85 × M85/M85	F$_1$	47	29		0.80 (2:1)
M85/M85 × m85/M85	F$_1$	79	0		–
m100/M100 × m100/M10	Self	80	68		0.97 (1:1)
m100/M100 × M100/M100	F$_1$	19	8		0.17 (2:1)
M100/M100 × m100/M100	F$_1$	112	0		–

[a]All χ^2 values indicate $P > 0.1$.

Interestingly, the *m31* and *m34* mutations were mapped between markers NGA112 and T20O10-1 at the bottom of chromosome 3 (Fig. 2A), where the auxin receptor gene *TIR1* is located (Dharmasiri et al., 2005a; Kepinski and Leyser, 2005). Moreover, the *tir1-1* roots were strongly resistant to PCIB (Fig. 3). To explore the possible allelism of these mutants with *tir1-1*, we sequenced the *TIR1* gene amplified from the *m31* and *m34* genomic DNA (Fig. 2B). In *m31*, we found a C-to-T point mutation on the second exon of the *TIR1* gene, which changes an Arg residue (Arg-220) to a stop codon. Similarly, the *TIR1* gene of *m34* has a G-to-A point mutation in the first exon, which changes a Cys residue (Cys-140) to Tyr. This Cys residue is conserved among TIR1/AFB proteins (Tan et al., 2007). Hence, *m31* and *m34* are new alleles of the *tir1* mutants. The *m85* and *m100* mutations were also mapped between markers NGA112 and T20O10-1. However, their male gametophyte-lethal phenotype, which has not been reported in any alleles of *tir1-1*, suggests that these mutations are located in genes other than *TIR1*.

The *aar2-1* mutant was isolated from the Versailles T-DNA population (N5509). The PCIB-resistant phenotype was inherited as semidominant and was linked to kanamycin resistance, indicating that the *aar2-1* mutation is caused by a T-DNA insertion. Thermal asymmetric interlaced-PCR, followed by sequence analyses for *aar2-1* genomic DNA, revealed that two copies of T-DNA are inserted as a right-border/right-border inverted repeat just downstream of the 3′ transcriptional termination site of the *AtCUL1* gene (*At4g02570* or *AXR6*), which encodes a scaffold subunit of the SCF ubiquitin ligase complex (Shen et al., 2002; Hellmann et al., 2003; Fig. 2C). To determine whether the defect of the *AtCUL1* gene confers PCIB resistance, a Salk line possessing a T-DNA insertion in the 19th exon of the *AtCUL1* gene (SALK_129379) was grown on GM containing 20 μM PCIB. Three of 11 seedlings showed PCIB resistance. The PCIB-resistant plants (designated as *aar2-2*) always showed segregation of PCIB-resistant and PCIB-sensitive seedlings in the next generation, indicating that the *aar2-2* mutant could be maintained only as a heterozygote (Fig. 2D). This is consistent with a previous finding that the homozygous null mutation in the *AtCUL1* gene is embryonic lethal (Shen et al., 2002). Thus, we concluded that the *AtCUL1* gene is required for normal sensitivity to PCIB. These results, along with identification of *tir1* alleles in the PCIB screening, confirmed that PCIB targets the upstream auxin-signaling pathway to inhibit root growth. The *aar5* mutation was also mapped close to *AtCUL1*. However, further mapping suggested that the *aar5* mutant is caused by a lesion in some other gene (data not shown).

The *aar3* and *aar4* mutations are located in the middle of chromosome 3 and the top half of chromosome 5, respectively (Fig. 2A).

The *aar* Mutants Are Resistant to Exogenously Applied 2,4-D

Identification of new alleles of *TIR1* and *AtCUL1* in the PCIB-resistant mutant series raises the possibility that other PCIB-resistant mutants also exhibit altered

A

3   4   5

M35, M36, — CIW5 (0.7)
    aar2   T10P11-1 (1.2)
    aar5

                   aar4 — RCI1B (3.3)
                      T24H18 (4.1)

aar1 — T6G15 (7.8)

aar3 — K5K13 (11.0)

M31, M34, — NGA112 (23.2)
M85, M100 — T20O10-1 (23.3)

B   *TIR1*

5' ◻ 3'

    M34   *M31*
  $(C^{140} > Y)$ $(R^{220} > stop)$

C   *AtCUL1*

5' ◻ 3'

          aar2-2   *aar2-1*
          T-DNA   T-DNA

D

WT

aar2-2/+

root length (cm)
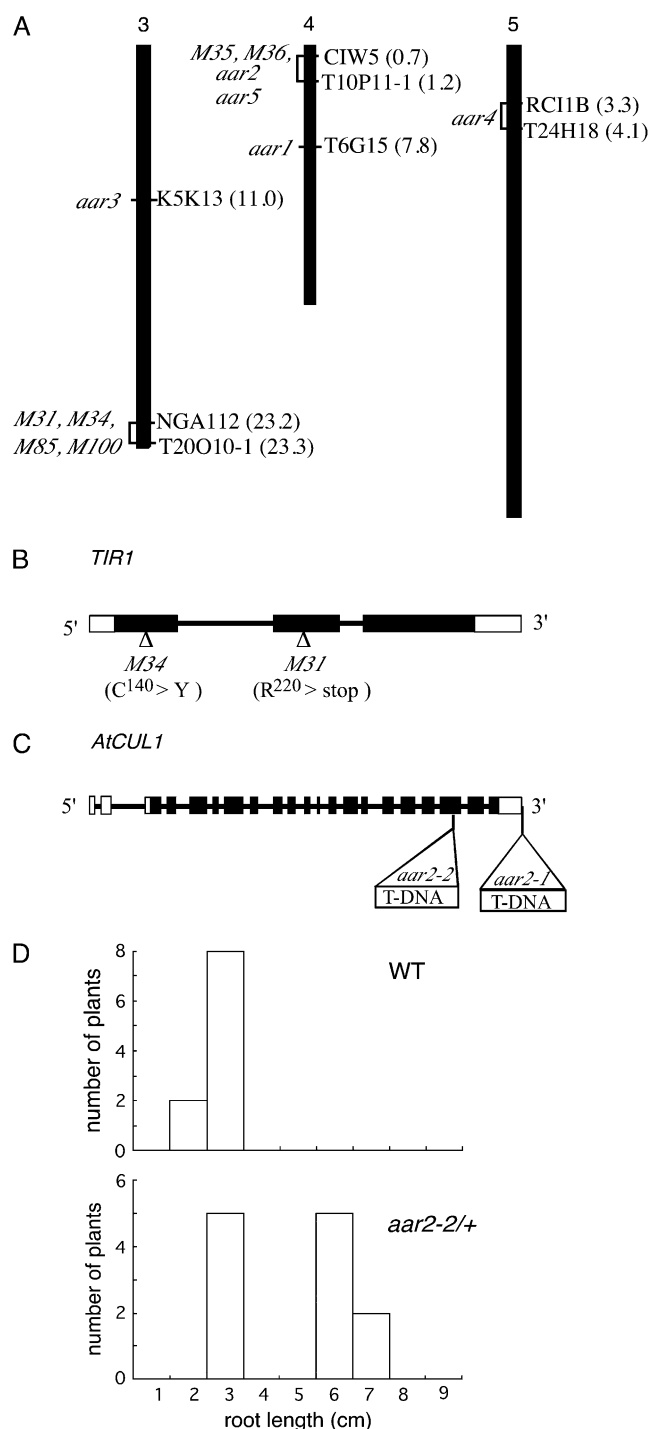
Figure 2. Mapping of the *aar* mutants and identification of mutation in *TIR1* and *AtCUL1* loci. A, Map position of PCIB-resistant mutations. Approximate Arabidopsis Genome Initiative map positions (Mb) of mapping markers are shown in parentheses to the right of each chromosome. The interval to which each PCIB mutant maps is shown to the left of the chromosomes. For *aar3-1*, no recombinants were identified from 826 chromosomes for markers K5K13-8, K5K13-9, and K5K13-2. *m31, m34, m85,* and *m*100 have 1/396, 1/108, 1/20, and 3/104 recombinants at NGA112 and 0/792, 0/110, 0/20, and 0/150 recombinants at T20O10-1, respectively. *aar5, m35,* and *m36* have 6/78, 1/40, and 3/60 recombinants at CIW5-1 and 4/120, 0/86, and 0/60 recom-

auxin sensitivity. To explore this hypothesis, we employed a root growth assay for *aar3-1, aar4,* and *aar5,* along with auxin-signaling *tir1-1* (Ruegger et al., 1998) and auxin-transport *aux1-7* (Marchant et al., 1999) mutants on media containing PCIB, 2,4-D, and IAA. No severe growth defect was observed in the primary root in the *aar* mutants in unsupplemented medium (Fig. 3A). PCIB at a concentration of 20 μM inhibited root growth in the wild type and *aux1-7* (Fig. 3B). In contrast, the *tir1-1* and *aar* mutants showed a significant resistance to PCIB-induced root growth inhibition (Fig. 3, B and C). In the auxin root growth assay, all three *aar* mutants were clearly less sensitive than the wild type to 100 nM 2,4-D (Fig. 3D). However, we did not observe a clear difference between the wild type and the *aar* mutants in the root growth assay on IAA medium (Fig. 3E). Only *aar5* showed a slight resistance to IAA ($P < 0.01$ at 50 and 100 nM IAA; Fig. 3E).

The *aar* seedlings, in addition to showing root growth resistance to exogenous applied 2,4-D, also showed other auxin-linked morphological abnormalities. For example, hypocotyls were shorter in *aar3-1* and *aar5* and longer in *aar4* than in the wild type ($P < 0.001$ for all; Fig. 3, F and G). The significantly lower number of lateral roots in *aar4* ($P < 0.001$) is another example of an auxin-related phenotype (Hobbie and Estelle, 1994; Woodward and Bartel, 2005; Fig. 3H). Soil-grown plants of the *aar* mutants are visually indistinguishable from those of the wild type grown under the same conditions, except that the *aar4* plants have longer leaves (Fig. 3I). Mature plants of the *aar* mutants are also similar to those of the wild type in plant height, the number of lateral branches, inflorescences, or siliques, or distance between siliques (Table III).

Positional Cloning of the *AAR3* Gene

As demonstrated above, all the PCIB-resistant mutants showed 2,4-D resistance or auxin-related phenotypes, and some of them were found to have mutations in auxin-signaling genes such as *TIR1* or *AtCUL1*. Thus, it is possible that cloning of the remaining *AAR* genes will identify novel loci for auxin signaling. To this end, we decided to clone the gene responsible for *aar3* phenotypes that include resistance to both PCIB- and 2,4-D-induced root growth inhibition but wild-type sensitivity to the native auxin IAA (Fig. 3, D and E). Subsequent analyses revealed that *aar3-1* roots had wild-type sensitivity to other growth regulators, such as 4-indole-3-butyric acid (IBA), 6-benzyladenine, abscisic acid, methyl jasmonate, and 1-aminocyclopropane-1-carboxylic acid, and to gravity stimulus (Fig. 4).

binants at T10P11-1, respectively. *aar4* has 1/72 recombinants at both RCI1B and T24H18 markers. B, Location of the *m31* and *m34* mutation sites in the *TIR1* gene. Black and white boxes indicate exons in translated and untranslated regions, respectively. Lines indicate introns. C, Positions of T-DNA insertions in *aar2* mutants in the *AtCUL1* gene. D, Distribution of root length of wild-type and *aar2-2* heterozygous seedlings germinated and grown vertically on 20 μM PCIB for 14 d.

Figure 3. Phenotype of the *aar* mutants. A and B, Photographs of 3-d-old seedlings of *aar* mutants grown vertically for 8 d under white light on GM-MES medium without (A) or with (B) 20 μM PCIB. Two seedlings are shown for each mutant. C to E, Response to PCIB (C), 2,4-D (D), and IAA (E) in *aar* mutants. Seeds were germinated on GM-MES medium and grown under white light for 3 d. Germinated seedlings were transferred to media containing chemicals at indicated concentrations. Five days later, new root growth was measured and plotted as a percentage of root growth on medium without chemicals. Error bars represent SDs of the means of 12 to 14 seedlings. F, Seedlings grown horizontally on GM-MES for 4 d under white light at 23°C. Two seedlings are shown for each. G and H, Hypocotyl length (G) and number of lateral roots (H) of 11-d-old seedlings. For lateral roots, only visible primordia that emerged from the main root were counted. Error bars represent SDs of the means of 12 to 14 seedlings. I, Comparison of morphology of rosette leaves of the wild type and *aar4*. Plants were grown for 35 d on a 1:1 mixture of vermiculite and Metromix 350 (Scotts-Sierra Horticultural Products) without any supplementation at 23°C in a growth chamber under a 14-h-light and 10-h-dark regime.
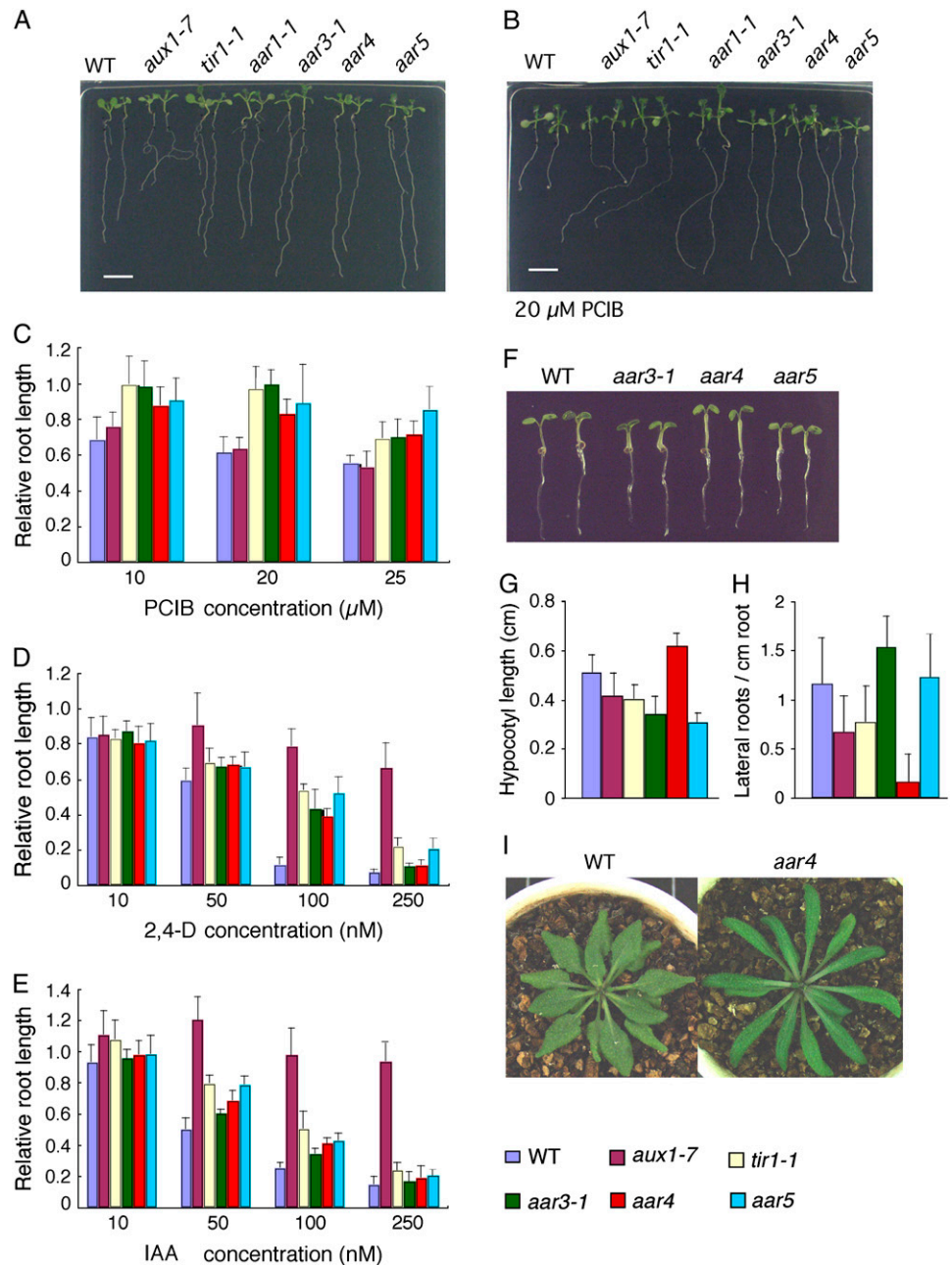
Fine mapping narrowed the location of the *aar3-1* mutation down to a 71-kb region between the markers MYI13-1 (three recombinants/816 chromosomes) and K5K13-4 (2/826) on chromosome 3. Sequence analyses of long PCR products of *aar3-1* genomic DNA revealed a G-to-A mutation in the splice donor site of the third intron of the *At3g28970* gene, which probably causes aberrant RNA processing and leads to a premature stop codon in the *AAR3* translational product. The mutation site and the presumed amino acid sequence of the *aar3-1* gene are illustrated in Figure 5A.

To clarify whether the defect in the *At3g28970* gene is responsible for the *aar3* phenotypes, we obtained T-DNA insertion lines, SALK_148316 and SALK_140306, generated by the Salk Institute Genomic Analysis Laboratory (Alonso et al., 2003). We found PCIB-resistant seedlings in both seed populations and established homozygous lines for PCIB resistance. Crossing of homozygous PCIB-resistant plants from the SALK_148316 and SALK_140306 lines to *aar3-1* resulted in PCIB-resistant F$_1$ seedlings, indicating that both lines are allelic to *aar3-1* (data not shown). Hence, we designated them *aar3-2* and *aar3-3*, respectively. Although neither *aar3-2* nor *aar3-3* seedlings exhibited kanamycin resistance, T-DNA insertion sites in the *At3g28970* gene were confirmed by sequencing the T-DNA left-border

Table III. *Morphological characteristics of mature (75-d-old) wild-type and aar mutants*[a]

Parameter	Wild Type	aar3-1	aar4	aar5
Plant height (cm)	25.6 ± 3.8	27.8 ± 5.1	30.6 ± 4.0	25.7 ± 3.3
No. lateral branches	3.5 ± 1.1	4.1 ± 0.7	3.1 ± 0.3	3.4 ± 0.7
No. inflorescences	6 ± 2.8	8 ± 2.5	7.5 ± 2.1	6.3 ± 2.8
No. siliques	81.2 ± 21.0	90.0 ± 31.0	104.0 ± 20.2	75.6 ± 20.0
Distance of siliques	0.8 ± 0.1	0.71 ± 0.1	0.76 ± 0.1	0.78 ± 0.2

[a]Means ± SD (n = 10–12 plants) are shown.

region amplified from *aar3-2* and *aar3-3* genomic DNA by thermal asymmetric interlaced-PCR (Fig. 5A). Furthermore, the primary roots of homozygous *aar3-2* seedlings grown in 2,4-D medium were longer than those of the wild type (Fig. 5D). The primary roots of homozygous *aar3-3* seedlings grown in 2,4-D medium were also longer than those of the wild type (data not shown). For further clarification, we examined *At3g28970* gene expression by reverse transcription (RT)-PCR and RNA hybridization using total RNA (Fig. 5, B and C; Supplemental Fig. S1). *At3g28970* gene expression was similar to that in the wild type, *tir1-1*, *aux1-7*, *aar4*, and *aar5*, as expected, while mRNA accumulation was considerably reduced in the *aar3* mutants (Fig. 5, B and C; Supplemental Fig. S1). Finally, we introduced 6.6-kb DNA fragments containing only the *At3g28970* gene into *aar3-1* and *aar3-2*, and rescued PCIB-sensitive seedlings in the T₂ population of *aar3-1* (eight lines per nine T₁ lines) and *aar3-2* (all 12 T₁ lines; Fig. 5, A and E). These results confirmed that the *At3g28970* gene is responsible for the *aar3* mutant phenotype.

The *At3g28970* gene (*AAR3*) encodes an expressed protein comprised of 295 amino acid residues with unknown function. The AAR3 protein contains bipartite and pattern 7 nuclear localization signals (NLSs; Abel and Theologis, 1995; Wang et al., 2003; Zheng et al., 2004; Thakur et al., 2005; Fig. 6A). Transient expression analyses of AAR3 fused to the C terminus of yellow fluorescent protein (YFP-AAR3) or the N terminus of cyan fluorescent protein (AAR3-CFP) confirmed the predicted nuclear localization of AAR3 (Fig. 6B; Supplemental Fig. S2). BLAST searches indicated that the middle region (amino acid nos. 72–177) of the AAR3 protein is characterized by a DUF298 domain of unknown function (PF03556), and has homology with conserved proteins annotated as DCN-1 (-like), RP42 (-like), or Leu zipper-like, which are widely present in both plants and animals (Fig. 6C). High conservation of the amino acid sequences in the DUF298 domain (amino acid nos. 160–172 in AAR3) among these proteins suggests that AAR3 and related proteins have important biological functions.

The amino acid sequence of the *AAR3* gene, which shares homology with the DCN-1 protein, raises a possibility that AAR3 is involved in SCF^TIR1-mediated proteolysis and may regulate auxin-induced gene expression. To characterize the effect of the *aar3* mutation on auxin-signaling events, we examined the expression of *HS::AXR3NT-GUS* and *DR5::GUS* in both wild-type and *aar3-2* backgrounds. However, no significant difference in auxin-regulated GUS activity was observed between the wild type and *aar3-2* (Supplemental Fig. S3).

DISCUSSION

In this work, we isolated 11 independent mutants whose root growth was resistant to PCIB. At least three of these mutants were defective in known auxin-signaling genes, *TIR1* (*m31* and *m34*) and *AtCUL1* (*aar2*). Both genes are key components of auxin perception and auxin-dependent ubiquitin-mediated proteolysis (Gray et al., 1999; Hellmann et al., 2003). In addition, other antiauxin-resistant mutants (*aar3*, *aar4*, and *aar5*) are resistant to the synthetic auxin 2,4-D. Molecular characterization of the *aar3* mutant suggests that the *AAR3* gene encodes a DCN1-like protein and regulates the response to 2,4-D in Arabidopsis roots.

Auxin resistance in root growth is generally associated with auxin transport or auxin signaling (Hobbie and Estelle, 1994). The present results suggest that *aar* mutants are defective in auxin-related signaling rather than auxin transport. First, roots of the auxin-transport mutant *aux1-7*, when grown vertically in unsupplemented medium, were completely agravitropic (Fig. 3A). In contrast, roots of all three *aar* mutants were normal, like that of the wild type or *tir1-1*, under the same growth conditions. Generally, it is assumed that the gravity response in root is tightly regulated by the polar auxin-transport system and that any perturbation of this system results in agravitropic root, as confirmed by previous works (Luschnig et al., 1998; Müller et al., 1998; Marchant et al., 1999). The normal gravity response that we observed in *aar* roots confers that the mutations did not affect the auxin-transport system. Second, PCIB does not require known auxin influx or efflux carrier proteins to enter or exit from the cell as was shown by analyzing *aux1* and *eir1-1* mutants, which are sensitive to PCIB (Fig. 3B; Oono et al., 2003). Finally, sequence motifs of the protein encoded by the *AAR3* gene and the identification of *TIR1* and *AtCUL1* alleles in PCIB screening suggest that PCIB targets the signaling component.

AAR3, the gene responsible for the *aar3* phenotype, encodes a novel protein. The protein shows homology with the DCN-1 protein family through DUF298

Figure 4. Responses of roots of the wild type and *aar3-1* to IBA, other classes of phytohormones, and gravity. A to E, Germinated seedlings (3 d old) were transferred to media containing IBA (A), abscisic acid (ABA; B), 6-benzyladenine (BA; C), 1-aminocyclopropane-1-carboxylic acid (ACC; D), and methyl jasmonate (Me-JA; E) and grown vertically under white light. Elongated root length was measured after 5 d of incubation. Values are expressed as a percentage of root growth without hormones for each genotype. Each data point represents the mean ± SD of 12 to 14 seedlings. F, Distribution of root growth direction of the seedlings after 3 d of stimulation at 135° to the vertical (*n* = 25 for the wild type and 26 for *aar3-1*). Three-day-old seedlings were transferred to fresh GM-MES medium, given 135° gravity stimulus, and incubated in the dark for 3 d. The arrows indicate the vector of gravity before (1) and after (2) the commencement of gravity stimulus. The angles were grouped into 12 classes and expressed as percentage in a wheel diagram. [See online article for color version of this figure.]
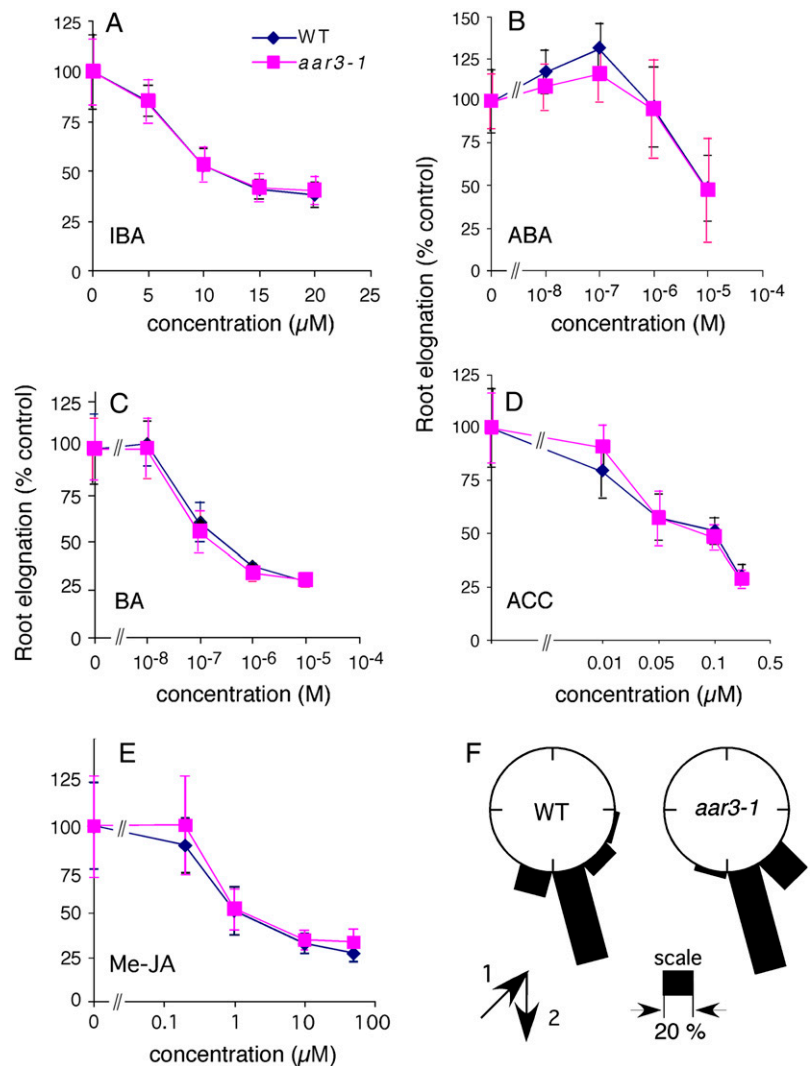
(domain of unknown function 298) that contains a Leu zipper-like region. A DCN-1 protein was recently identified by large-scale RNAi screening for loss of CUL3 function in *Caenorhabditis elegans* and has been shown to interact with ubiquitin and the ubiquitin-like protein Nedd8 (Kurz et al., 2005). DCN-1 and its yeast homolog, Dcn1p, bind to the *C. elegans* CUL3 protein and Cdc53p, a CUL1 homolog in yeast, respectively, and facilitate cullin neddylation both in vitro and in vivo (Kurz et al., 2005). The DCN-1 protein consists of an amino-terminal UBIQUITIN-ASSOCIATED (UBA)-like domain and a carboxyl-terminal DUF298 domain. The UBA-like domain of DCN-1 directly and specifically interacts with ubiquitin, while it interacts only weakly with Nedd8, raising the possibility that the DUF298 domain of this protein is involved in binding to the CULLIN and Nedd8 proteins, although no clear evidence for this has been presented (Kurz et al., 2005). Because AAR3 does not possess a UBA-like domain, elucidation of AAR3 interaction with the CULLINs and Rub1 proteins, the equivalent of Nedd8 in Arabi-

dopsis, should clarify the functional significance of the DUF298 domain in cullin modification. In Arabidopsis, RUB/Nedd8 modification of CUL1 is required for auxin signaling and its disruption confers auxin resistance in the root elongation assay (del Pozo et al., 2002; Dharmasiri et al., 2003). This, together with the fact that mutations were found in the *TIR1* and *AtCUL1* genes in other PCIB-resistant mutants, suggests that AAR3 may also be involved in the regulation of the SCF-dependent protein degradation system. However, our data indicated that loss of AAR3 did not have any profound effect on the stability of AUX/IAA protein degradation or auxin-induced gene expression (Supplemental Fig. S3). A possible explanation of these unexpected results is that AAR3 does not participate in the SCF^{TIR1} pathway. Alternatively, the other two *AAR3*-like genes present in the Arabidopsis genome (Kurz et al., 2005) may have functionally redundant roles in auxin signaling in Arabidopsis, which would explain why the single mutant shows a weak phenotype. Further analysis of double or triple mutants of
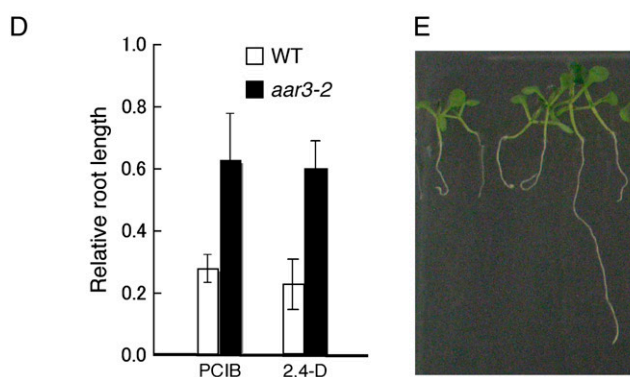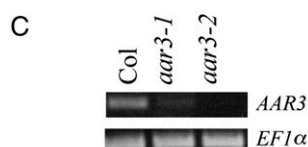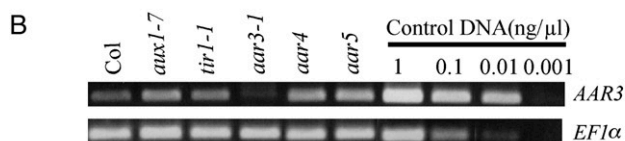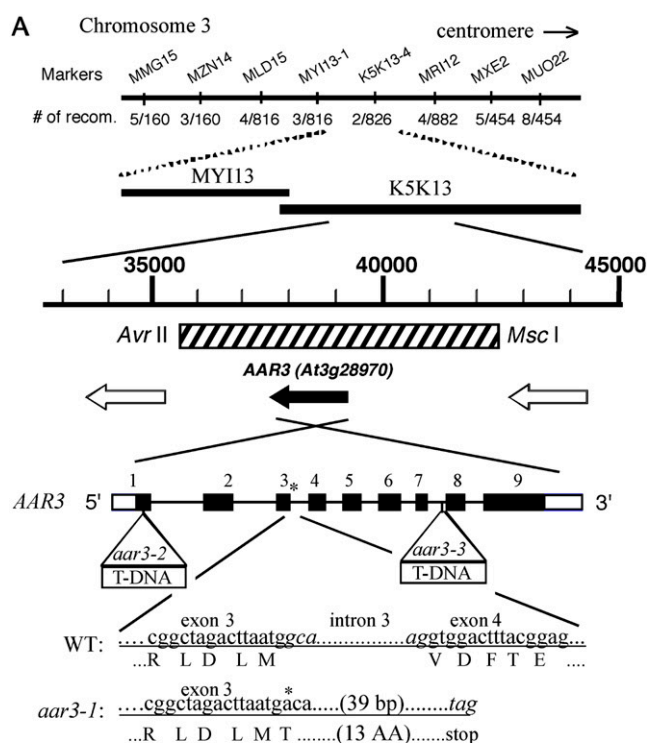
Figure 5. Molecular cloning of the *AAR3* gene. A, Fine mapping with the PCR-based markers MMG15-2, MZN14-1, MLD15-1, MYI13-1, K5K13-2, MRI12-5, MXE2-3, and MUO22-1, which are located at the MYI13 and K5K13 regions on chromosome 3. The position of the 6.6-kb DNA fragment used for the complementation test is indicated with a hatched box. Open reading frames in this region were shown with black (for *AAR3*) and white arrows (for other open reading frames). Black and white boxes of *AAR3* indicate exons in translated and untranslated regions, respectively. Lines indicate introns. The position of the mutation in *aar3-1* is indicated with an asterisk, and the positions of

these genes will clarify the mode of action of these DCN1-like proteins in Arabidopsis.

The auxin response analyses suggested that the *aar3* root is clearly resistant to 2,4-D, while the IAA response is subtle. The previously reported *aar1* mutants also show similar auxin response (Rahman et al., 2006). One possible explanation why *aar3* is profoundly resistant to 2,4-D could be that 2,4-D- and IAA-signaling pathways are partially distinct as argued by Rahman et al. (2006). Interestingly, as reported by Woodward et al. (2007), we also observed that the *tir1-1* mutant showed great resistance to 2,4-D but rather weak resistance to IAA. It is now well recognized that several gene families function redundantly in auxin-signaling pathways in plant cells. For example, Arabidopsis has at least five auxin or auxin-related receptors (TIR1 and AFBs; Dharmasiri et al., 2005b; Walsh et al., 2006). Although a recent crystal structural analysis of TIR1 protein suggested that 2,4-D binds to TIR1 in a manner similar to IAA (Tan et al., 2007), it is possible that each receptor has a different affinity for different auxin molecules and contributes differentially to activate downstream events of auxin signaling. Indeed, seedlings harboring a mutation in *AFB5* are resistant to synthetic auxinic herbicide picolinates but not to 2,4-D (Walsh et al., 2006). The *ecr1-1* mutant of Arabidopsis, which was isolated by screening for resistance to indole-3-propionic acid, also exhibited differential responses to different auxin compounds (Woodward et al., 2007). Thus, chemical specificity in auxin signaling might be the reason for the preferential resistance to 2,4-D in *aar3* mutants.

In this study and our previous study (Rahman et al., 2006), we have isolated more than six PCIB-resistant loci, including alleles of *TIR1* and *AtCUL1*, and have shown that mutations in the same gene give rise to resistance to both auxin (at least 2,4-D) and PCIB. The straightforward explanation for their common behavior is that both PCIB and auxin inhibit root growth by the same response pathway. We previously showed that PCIB antagonized exogenously applied auxin by

the T-DNA insertion in *aar3-2* and *aar3-3* are indicated with open triangles. *aar3-1* has a G-to-A mutation at the first base of the third intron, which may prevent normal splicing and result in generation of a truncated product. Nucleotides in the third intron in the wild type and the predicted stop codon in *aar3-1* are shown in italics. B and C, The steady-state levels of the *AAR3* transcript in various mutants analyzed by RT-PCR. Same volume (1 μL) of control DNA with different concentration (1 ng μL^{-1}, 0.1 ng μL^{-1}, 0.01 ng μL^{-1}, or 0.001 ng μL^{-1}) was used in the PCR reaction. D, Relative root length of *aar* mutants grown on PCIB or 2,4-D. Seeds were germinated on GM-MES medium containing 20 μM PCIB or 40 nM 2,4-D, and grown vertically under white light for 10 d. Root growth was measured and plotted as a percentage of root growth on control medium without the growth regulators. Error bars represent SDs of the means of at least 16 seedlings. E, Segregation of PCIB-sensitive seedlings in the T$_2$ population of a transgenic *aar3-2* line (line 12) transformed with the 6.6-kb fragment indicated as a hatched box in A. The seedlings were germinated and grown for 9 d on 20 μM PCIB. [See online article for color version of this figure.]

A

```
  1  MDSSPVSARFDIFEIYRRFCAIRSGQQLCNKKPCDGEESQRFNLSKEAITQLLYLVENKF

 61  QARNSIFDELFKLMSRLDLMVDFTEFTCFYDFVFFMCRENGQKNITISRAITAWKLVLAG

121  RFRLLNRWCDFIEKNQRHNISEDTWQQVLAFSRCVHENLEGYDSEGAWPVLIDDFVEHMY

181  SILGPNKDTSLFCKCGDTESESCLYQEDEHHKDYRRPHTGLRNIPGLKRKTSKKNDEEEE

240  DEDEEVLETQNSSSLLNFKRIKTSNSPRCSSKSPCSIERSLSQGFASLLSTGDKP
```

B

C
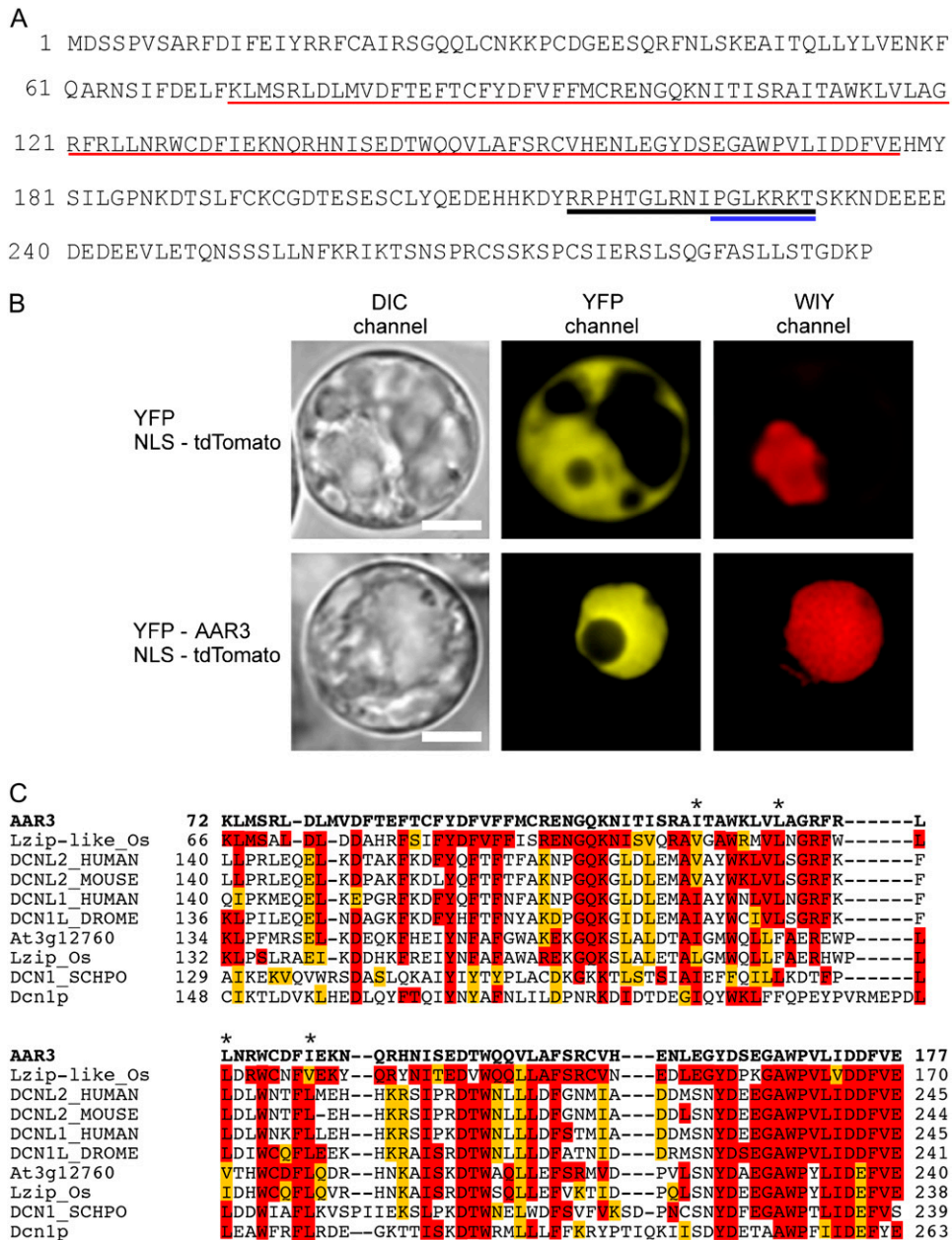
Figure 6. Amino acid sequence of the AAR3 protein and alignment of the DUF298 domain region with other AAR3-like proteins. A, The *AAR3* proteins are composed of 295 amino acid residues. The DUF298 domain is indicated with a red underline. NLSs bipartite (RRPHTGLRNIPGLKRKT) and pattern 7 (PGLKRKT) are shown by black and blue underlines, respectively. B, Nuclear localization of YFP-AAR3 in Arabidopsis protoplasts. Shown are protoplasts of Arabidopsis T87 suspension-cultured cells coexpressing *35S*::*YFP* and *35S*::*NLS-tdTomato* (top panels), and *35S*::*YFP-AAR3* and *35S*::*NLS-tdTomato* (bottom panels). YFP-AAR3-associated fluorescence is localized in the nucleus, but nonfused YFP fluorescence is distributed in both the nucleus and the cytosol. NLS-tdTomato was used as the nuclear marker and its fluorescent signal was captured in the WIY channel. Bars = 10 nm. C, ClustalW alignment of the DUF298 domains of AAR3 and AAR3-like proteins. The amino acid sequence (amino acid nos. 72–177, shown in red underlines in A) of the DUF298 domain of the AAR3 protein (bold letters in the top line) was used for alignment with a Leu zipper-like protein of *Oryza sativa* (NP_001060359), DCN1-like protein 2 of human (Q6PH85) and mouse (Q8BZJ7), DCN1-like protein 1 of human (Q96GG9) and *Drosophila* (Q9VUQ8), At3g12760 protein from Arabidopsis (AAK93603), Leu zipper protein of *O. sativa* (BAD38167), DCN-1 of *Schizosaccharomyces pombe* (Q8WZK4), and Dcn1p of *Saccharomyces cerevisiae* (NP_013229). Amino acid residues identical and similar to the AAR3 sequence are colored with red and orange, respectively. Asterisks show Leu residues in the putative Leu zipper-like domain.
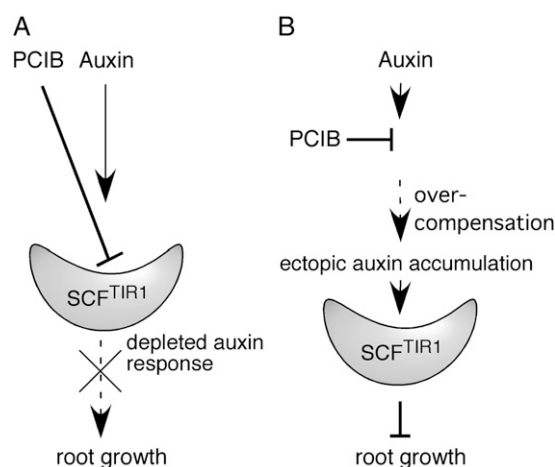
Figure 7. Proposed model for PCIB resistance of the *tir1* and *atcul1* mutants and PCIB-dependent root growth inhibition. A, PCIB inhibits SCF^{TIR1} activity and reduces auxin response. Depletion of auxin response directly results in root growth inhibition. B, PCIB indirectly promotes ectopic auxin accumulation in the root, which causes root growth inhibition through SCF^{TIR1}-dependent auxin signal transduction.

inhibiting the upstream auxin-signaling pathway, suggesting that PCIB reduces the cellular response to auxin (Oono et al., 2003). The structural similarity of PCIB to 2,4-D and the fact that the alleles of *TIR1* and *AtCUL1* are PCIB resistant imply that PCIB interacts with the SCF^{TIR1} complex and down-regulates the normal auxin response (Fig. 7). Because the cellular auxin response plays a key role in regulating the organization of root meristem and root growth (e.g. Sabatini et al., 1999; Sibout et al., 2006), roots do not grow properly in the weakened auxin-signaling condition caused by PCIB (Fig. 7A). Alternatively, root growth inhibition by PCIB may be a secondary consequence of ectopic overaccumulation of auxin. This idea is supported by the findings that (1) PCIB does not immediately inhibit root growth, and (2) long-term treatment of PCIB causes changes in root morphology (such as swelled root tips) and the *DR5::GUS* expression pattern as well as an increase in auxin levels. Because auxin homeostasis is regulated, at least in part, through negative feedback by auxin-inducible proteins such as Aux/IAA transcriptional repressors and GH3 auxin-conjugating enzymes (Leyser, 2002; Staswick et al., 2005), the reduction of the cellular response to internal auxin by PCIB could abolish this feedback regulation and consequently lead to overcompensation with an ectopic cellular auxin response or accumulation that ultimately inhibits root growth (Fig. 7B).

In conclusion, we have shown that the use of PCIB in genetic studies facilitates the isolation of novel auxin-related signaling factors. Further, we have identified a gene, *AAR3*, which encodes a DCN1-like protein, as a new regulator of the 2,4-D response. Future investigations of the biochemical functions of AAR3 and previously identified SMAP proteins (Rahman

et al., 2006) will provide a better understanding of auxin-related signaling pathways.

MATERIALS AND METHODS

Plant Materials

All transgenic and mutant lines, except QC marker lines and *aar2-1*, were derived from Arabidopsis (*Arabidopsis thaliana* L. Heynh), Columbia-0 ecotype. QC marker lines and *aar2-1* are Wassilewskija ecotype. Transgenic lines containing *DR5::GUS* and QC marker lines are described by Ulmasov et al. (1997) and Sabatini et al. (1999), respectively. Landsberg *erecta* was used for genetic mapping of the *aar* mutants. The auxin-resistant mutants *tir1-1* (Ruegger et al., 1998), *aar2-2* (SALK_129379), *aar3-2* (SALK_148316), and *aar3-3* (SALK_140306) and the BAC clones were obtained from the Arabidopsis Biological Resource Center (Alonso et al., 2003). *aar1-1* and *aux1-7* are described by Rahman et al. (2006) and Marchant et al. (1999), respectively.

Seven (*aar3-1*, *aar4*, *aar5*, *m31*, *m34*, *m35*, and *m36*), three (*aar1*, *m85*, and *m100*), and one (*aar2-1*) mutant lines were isolated from populations mutagenized by EMS, ion-beam irradiation, and insertion of a T-DNA, respectively. Procedures for isolating the *aar* mutations are described in Supplemental Materials and Methods S1.

Growth Analyses

Seeds were surface-sterilized and plated on GM (half-strength Murashige and Skoog salts, 1% [w/v] Suc, and 0.5 g L^{-1} MES, pH 5.8, containing 1× B5 vitamins and 0.8% [w/v] Bacto agar) in rectangular plates. For synchronous germination, the seeds were kept in the dark for 2 d at 4°C. Then, the plates were transferred to growth chamber and oriented vertically at 23°C under continuous light at an intensity of 20 to 30 μE m^{-2} s^{-1} supplied by fluorescent bulbs (FL 20SS-BRN/18; Toshiba). Percentage of root growth inhibition was calculated relative to root growth on media without growth regulators. Plant growth regulators were dissolved in dimethyl sulfoxide at a concentration 1,000 times greater than needed. The same amount of dimethyl sulfoxide was added to the control treatments. IAA, IBA, and PCIB were purchased from Sigma. Other chemicals were from Wako Pure Chemicals Industries, Ltd. To observe morphology of plants grown on soil (for Fig. 3I), seedlings were grown in growth chambers (NK system: Type-100-RDS; model: 01 K-D6P) at 23°C. To characterize mature plants (for Table III), the seedlings were grown in a greenhouse, and the number of lateral roots, siliques, lateral branches, and inflorescences were counted by eye. Lengths between two siliques were determined by measuring the total shoot length in each plant. Unless otherwise specified, the *F* test (Sokal and Rohlf, 1995) was used to test for significant differences.

GUS histochemical analysis was performed as described by Oono et al. (2003). Starch granules were visualized and tissues were cleared for microscopic analysis as described by Willemsen et al. (1998).

Quantification of Endogenous IAA in the Root Tip

For measuring free IAA in the root tip, the terminal 3 mm and 5 mm of primary roots were excised from 200 5-d-old and 10-d-old light-grown seedlings, respectively. Of each set of root tips, 140 root tips were immediately frozen in liquid nitrogen and used for IAA extraction. The remaining 60 root tips of each set were used for measuring fresh weight. IAA was extracted and quantified by gas chromatography single-ion-monitoring mass spectrometry as described by Tian et al. (2004).

Genetic Characterization of the *aar* Mutants

Procedures for mapping *aar* mutations and positional cloning of the *AAR3* gene are described in Supplemental Materials and Methods S1 and Supplemental Table S1. For complementation analysis, the 6.6-kb DNA fragments containing the *At3g28970* gene with 3.1-kb 5′- and 1.7-kb 3′-flanking regions were isolated from the BAC clone K5K13 by digesting with *Avr*II and *Msc*I, followed by subcloning to the *Xba*I/*Sma*I site of pPZP121. The resulting plasmid was introduced into *Agrobacterium* GV3101 (MP90). Transformed *Agrobacterium* were selected on medium containing 40 μg mL^{-1} gentamycine sulfate and 75 μg mL^{-1} chloramphenicol. Arabidopsis was transformed by the

AAR3 Expression Analysis by RT-PCR

Total RNA was extracted from shoots of 12-d-old Arabidopsis using the method of Biswas et al. (2003) with minor changes. The tissues were dipped in liquid N_2 and ground to fine powders. The extract was treated with the RNase-free DNase (Qiagen) to remove contaminating DNA. cDNA was prepared from 1 μg of total RNA using a Transcriptor first-strand cDNA synthesis kit (Roche Diagnostics). One microliter of cDNA solution was used for PCR amplification.

The gene-specific primer pairs used for PCR of AAR3 cDNA were AAR3a (5′-gtgatggcgaagaatctcaaag-3′) and AAR3b (5′-taacctaaatctcccagccaaa-3′), which extend from the second to the fifth exon and yielded a 265-bp product for mRNA and an 800-bp product for the genomic sequence. The same volume (1 μL) of template cDNA was applied in a final PCR mixture. For quantitative control, an AAR3 cDNA fragment of known concentration was amplified as control to compare steady-state level of transcript.

Transient Expression Analysis in Arabidopsis Protoplasts

Transient expression vectors that contain YFP (pAVA554) and CFP (pAVA574) genes derived by the cauliflower mosaic virus 35S promoter (von Arnim et al., 1998; Fukamatsu et al., 2005) were used for the control experiments. Construction of 35S::YFP-AAR3, 35S::AAR3-CFP, and 35S::NLS-tdTomato is described in Supplemental Materials and Methods S1. Transient transformation was performed according to Satoh et al. (2004). CFP, YFP, and tdTomato signals were detected with standard CFP, YFP, and WIY filters (OLYMPUS), respectively.

Sequence data from this article can be found in the GenBank/EMBL data libraries under accession numbers At3g28970, NP_001060359, Q6PH85, Q8BZJ7, Q96GG9, Q9VUQ8, AAK93603, BAD38167, Q8WZK4, and NP_013229.

Supplemental Data

The following materials are available in the online version of this article.

Supplemental Figure S1. RNA hybridization analysis in the aar3 mutants.

Supplemental Figure S2. Nuclear localization of AAR3-CFP in Arabidopsis protoplast.

Supplemental Figure S3. Comparison of 2,4-D-induced protein degradation and gene expression in the wild type and aar3-2.

Supplemental Table S1. Description of new simple sequence length polymorphism/cleaved amplified polymorphic sequence markers used for aar3-1 mapping.

Supplemental Materials and Methods S1. Isolation and mapping of the aar mutants, RNA hybridization, and construction of the reporters for the transient assay.

LITERATURE CITED

Abel S, Theologis A (1995) A polymorphic bipartite motif signals nuclear targeting of early auxin-inducible proteins related to PS-IAA4 from pea (Pisum sativum). Plant J **8:** 87–96

Alonso JM, Stepanova AN, Leisse TJ, Kim CJ, Chen H, Shinn P, Stevenson DK, Zimmerman J, Barajas P, Cheuk R, et al (2003) Genome-wide insertional mutagenesis of Arabidopsis thaliana. Science **301:** 653–657

Armstrong JI, Yuan S, Dale JM, Tanner VN, Theologis A (2004) Identification of inhibitors of auxin transcriptional activation by means of chemical genetics in Arabidopsis. Proc Natl Acad Sci USA **101:** 14978–14983

Biswas KK, Neumann R, Haga K, Yatoh O, Iino M (2003) Photomorphogenesis of rice seedlings: a mutant impaired in phytochrome-mediated inhibition of coleoptile growth. Plant Cell Physiol **44:** 242–254

Clough SJ, Bent AF (1998) Floral dip: a simplified method for Agrobacterium-mediated transformation of Arabidopsis thaliana. Plant J **16:** 735–743

del Pozo JC, Dharmasiri S, Hellmann H, Walker L, Gray WM, Estelle M (2002) AXR1-ECR1-dependent conjugation of RUB1 to the Arabidopsis cullin AtCUL1 is required for auxin response. Plant Cell **14:** 421–433

Dharmasiri N, Dharmasiri S, Estelle M (2005a) The F-box protein TIR1 is an auxin receptor. Nature **435:** 441–445

Dharmasiri N, Dharmasiri S, Weijers D, Lechner E, Yamada M, Hobbie L, Ehrismann JS, Jurgens G, Estelle M (2005b) Plant development is regulated by a family of auxin receptor F box proteins. Dev Cell **9:** 109–119

Dharmasiri S, Dharmasiri N, Hellmann H, Estelle M (2003) The RUB/Nedd8 conjugation pathway is required for early development in Arabidopsis. EMBO J **22:** 1762–1770

Fukamatsu Y, Mitsui S, Yasuhara M, Tokioka Y, Ihara N, Fujita S, Kiyosue T (2005) Identification of LOV KELCH PROTEIN2 (LKP2)-interacting factors that can recruit LKP2 to nuclear bodies. Plant Cell Physiol **46:** 1340–1349

Gray WM, del Pozo JC, Walker L, Hobbie L, Risseeuw E, Banks T, Crosby WL, Yang M, Ma H, Estelle M (1999) Identification of an SCF ubiquitin-ligase complex required for auxin response in Arabidopsis thaliana. Genes Dev **13:** 1678–1691

Hayashi K, Jones AM, Ogino K, Yamazoe A, Oono Y, Inoguchi M, Kondo H, Nozaki H (2003) Yokonolide B, a novel inhibitor of auxin action, blocks degradation of Aux/IAA factors. J Biol Chem **278:** 23797–23806

Hellmann H, Hobbie L, Chapman A, Dharmasiri S, Dharmasiri N, del Pozo C, Reinhardt D, Estelle M (2003) Arabidopsis AXR6 encodes CUL1 implicating SCF E3 ligases in auxin regulation of embryogenesis. EMBO J **22:** 3314–3325

Hobbie L, Estelle M (1994) Genetic approaches to auxin action. Plant Cell Environ **17:** 525–540

Kepinski S, Leyser O (2005) The Arabidopsis F-box protein TIR1 is an auxin receptor. Nature **435:** 446–451

Kurz T, Ozlu N, Rudolf F, O'Rourke SM, Luke B, Hofmann K, Hyman AA, Bowerman B, Peter M (2005) The conserved protein DCN-1/Dcn1p is required for cullin neddylation in C. elegans and S. cerevisiae. Nature **435:** 1257–1261

Leyser O (2002) Molecular genetics of auxin signaling. Annu Rev Plant Biol **53:** 377–398

Luschnig C, Gaxiola RA, Grisafi P, Fink GR (1998) EIR1, a root-specific protein involved in auxin transport, is required for gravitropism in Arabidopsis thaliana. Genes Dev **12:** 2175–2187

Marchant A, Kargul J, May ST, Muller P, Delbarre A, Perrot-Rechenmann C, Bennett M (1999) AUX1 regulates root gravitropism in Arabidopsis by facilitating auxin uptake within root apical tissues. EMBO J **18:** 2066–2073

Müller A, Guan C, Galweiler L, Tanzler P, Huijser P, Marchant A, Parry G, Bennett M, Wisman E, Palme K (1998) AtPIN2 defines a locus of Arabidopsis for root gravitropism control. EMBO J **17:** 6903–6911

Oono Y, Ooura C, Rahman A, Aspuria ET, Hayashi K, Tanaka A, Uchimiya H (2003) p-Chlorophenoxyisobutyric acid impairs auxin response in Arabidopsis root. Plant Physiol **133:** 1135–1147

Rahman A, Nakasone A, Chhun T, Ooura C, Biswas KK, Uchimiya H, Tsurumi S, Baskin TI, Tanaka A, Oono Y (2006) A small acidic protein 1 (SMAP1) mediates responses of the Arabidopsis root to the synthetic auxin 2,4-dichlorophenoxyacetic acid. Plant J **47:** 788–801

Ruegger M, Dewey E, Gray WM, Hobbie L, Turner J, Estelle M (1998) The TIR1 protein of Arabidopsis functions in auxin response and is related to human SKP2 and yeast Grr1p. Genes Dev **12:** 198–207

Sabatini S, Beis D, Wolkenfelt H, Murfett J, Guilfoyle T, Malamy J, Benfey P, Leyser O, Bechtold N, Weisbeek P, et al (1999) An auxin-dependent distal organizer of pattern and polarity in the *Arabidopsis* root. Cell 99: 463–472

Satoh R, Fujita Y, Nakashima K, Shinozaki K, Yamaguchi-Shinozaki K (2004) A novel subgroup of bZIP proteins functions as transcriptional activators in hypoosmolarity-responsive expression of the ProDH gene in Arabidopsis. Plant Cell Physiol 45: 309–317

Shen WH, Parmentier Y, Hellmann H, Lechner E, Dong A, Masson J, Granier F, Lepiniec L, Estelle M, Genschik P (2002) Null mutation of AtCUL1 causes arrest in early embryogenesis in Arabidopsis. Mol Biol Cell 13: 1916–1928

Sibout R, Sukumar P, Hettiarachchi C, Holm M, Muday GK, Hardtke CS (2006) Opposite root growth phenotypes of hy5 versus hy5 hyh mutants correlate with increased constitutive auxin signaling. PLoS Genet 2: e202

Sokal RR, Rohlf FJ (1995) Biometry: The Principles and Practice of Statistics in Biological Research, Ed 3. W.H. Freeman and Company, New York

Staswick PE, Serban B, Rowe M, Tiryaki I, Maldonado MT, Maldonado MC, Suza W (2005) Characterization of an *Arabidopsis* enzyme family that conjugates amino acids to indole-3-acetic acid. Plant Cell 17: 616–627

Surpin M, Rojas-Pierce M, Carter C, Hicks GR, Vasquez J, Raikhel NV (2005) The power of chemical genomics to study the link between endomembrane system components and the gravitropic response. Proc Natl Acad Sci USA 102: 4902–4907

Tan XT, Calderon-Villalobos LIA, Sharon M, Zheng C, Robinson CV, Estelle M, Zheng N (2007) Mechanism of auxin perception by the TIR1 ubiquitin ligase. Nature 446: 640–645

Thakur JK, Jain M, Tyagi AK, Khurana JP (2005) Exogenous auxin enhances the degradation of a light down-regulated and nuclear-localized OsiIAA1, an Aux/IAA protein from rice, via proteasome. Biochim Biophys Acta 1730: 196–205

Tian CE, Muto H, Higuchi K, Matamura T, Tatematsu K, Koshiba T, Yamamoto KT (2004) Disruption and overexpression of auxin response factor 8 gene of Arabidopsis affect hypocotyl elongation and root growth habit, indicating its possible involvement in auxin homeostasis in light condition. Plant J 40: 333–343

Ulmasov T, Murfett J, Hagen G, Guilfoyle TJ (1997) Aux/IAA proteins repress expression of reporter genes containing natural and highly active synthetic auxin response elements. Plant Cell 9: 1963–1971

von Arnim AG, Deng XW, Stacey MG (1998) Cloning vectors for the expression of green fluorescent protein fusion proteins in transgenic plants. Gene 221: 35–43

Walsh TA, Neal R, Merlo AO, Honma M, Hicks GR, Wolff K, Matsumura W, Davies JP (2006) Mutations in an auxin receptor homolog AFB5 and in SGT1b confer resistance to synthetic picolinate auxins and not to 2,4-dichlorophenoxyacetic acid or indole-3-acetic acid in Arabidopsis. Plant Physiol 142: 542–552

Wang P, Wu P, Egan RW, Billah MM (2003) Identification and characterization of a new human type 9 cGMP-specific phosphodiesterase splice variant (PDE9A5): differential tissue distribution and subcellular localization of PDE9A variants. Gene 314: 15–27

Weijers D, Jürgens G (2004) Funneling auxin action: specificity in signal transduction. Curr Opin Plant Biol 7: 687–693

Willemsen V, Wolkenfelt H, de Vrieze G, Weisbeek P, Scheres B (1998) The *HOBBIT* gene is required for formation of the root meristem in the *Arabidopsis* embryo. Development 125: 521–531

Woodward AW, Bartel B (2005) Auxin: regulation, action, and interaction. Ann Bot (Lond) 95: 707–735

Woodward AW, Ratzel SE, Woodward EE, Shamoo Y, Bartel B (2007) Mutation of E1-CONJUGATING ENZYME-RELATED1 decreases RELATED TO UBIQUITIN conjugation and alters auxin response and development. Plant Physiol 144: 976–987

Yamazoe A, Hayashi K, Kepinski S, Leyser O, Nozaki H (2005) Characterization of terfestatin A, a new specific inhibitor for auxin signaling. Plant Physiol 139: 779–789

Zheng C, Brownlie R, Babiuk LA, van Drunen Littel-van den Hurk S (2004) Characterization of nuclear localization and export signals of the major tegument protein VP8 of bovine herpesvirus-1. Virology 324: 327–339